

MULTILEVEL ADAPTATION FOR AUTONOMOUS MOBILE ROBOT FORMATIONS

Sanjay S. Joshi*

Member, AIAA[†]

Jet Propulsion Laboratory, California Institute of Technology
Pasadena, California

ABSTRACT

This paper studies adaptive behavior within multi-agent autonomous robot formation-keeping. The goal of the research is to develop control laws for each robot in a formation such that the formation as a whole maintains a certain geometric configuration in the face of changing terrain conditions and actuator constraints. It is a main result of this paper that adaptation can occur at several different levels in a formation control architecture; just as a single robot may adapt to a new environment, a robot-formation as a whole may also adapt to a new environment. Terrain uncertainty and related actuator saturation are identified as important limitations to formation-keeping in uncertain environments. In order to account for terrain uncertainty, individual robots are equipped with parameter estimators to allow implementation of direct adaptive control. Using these adaptive controllers, it is shown that formation error reduces to zero under non-saturated conditions. Actuator saturation brings new challenges to formation-keeping. It is shown that rough terrain can easily lead to actuator saturation. For this case, a new ethological control scheme is introduced. It is shown that in this case the entire formation adapts to the weakest robot.

INTRODUCTION

This paper studies adaptive behavior within multi-agent autonomous robot formation-keeping. The goal of the research is to develop control laws for each robot in a formation such that the formation as a whole maintains a certain geometric configuration in the face of changing terrain conditions and actuator constraints. The motivation for this work is robotic cooperation necessary for tasks relating to robotic outposts [1] or robotic exploration. In these cases, the environment the robots encounter will not be known for certain and is likely to change with time and distance traveled. For example, the friction of the terrain that the robots traverse will likely change with time. Furthermore, each robot in the formation may experience a different terrain friction. Therefore, it will be important to account for this interaction with the environment. In addition, actuator saturation is closely linked with terrain impedance. A more difficult terrain leads to greater control forces, which have more chance of saturating.

For this study, we employ dynamic systems theory as a framework. The mathematical dynamic systems theory framework for general adaptive robotics problems has been advocated by Beer [2]. Dean and Wellman [3] have also discussed robotics from a dynamic systems perspective. Many times controllers are constructed based on predicted behavior of the machine or explicit models of both the machine and its environment. These predictions and models are always uncertain to some degree. Therefore, some controllers are designed to change on-line based on actual measurements of the machine and/or environment. This is known as adaptive control. It is a main result of this paper that adaptation can occur at several different levels in a formation control architecture; just as a single robot may adapt to a new environment, a robot-formation

*sanjay.s.joshi@jpl.nasa.gov

[†]Copyright ©2000 American Institute of Aeronautics and Astronautics, Inc. No copyright is asserted in the United States under Title 17, U.S. Code. The U.S. Government has a royalty-free license to exercise all rights under the copyright claimed herein for Government Purposes. All other rights are reserved by the copyright owner.

as a whole may also adapt to a new environment.

PREVIOUS WORK

Formation-keeping has received considerable recent interest in the robotics community as part of the more general field of cooperating multiple autonomous agents. Most of the work in formation-keeping has focused on the study of different control architectures whose aim is to coordinate formation-keeping, goal achievement, and obstacle avoidance. Almost all of these studies employ linguistic-based or rule-of-thumb controllers for robot implementation. Parker [4] [5] studied line formation-keeping within the subsumption software architecture. She found that in general local plus global information-sharing helps formation maintenance and goal achievement in the subsumption architecture. Balch and Arkin [6] also studied line formation-keeping, but extended Parker's studies to include diamond, wedge, and column formations. In addition, they studied a behavioral motor schema approach which, unlike Parker's subsumption approach, allowed simultaneous behavior of formation-keeping, goal achievement, and obstacle avoidance tasks. Mataric [7] has studied general emergent group behavior. Her work has aimed to combine several "basis" behaviors such as avoidance and dispersion into complex emergent group behaviors such as flocking. In all the previously mentioned studies, issues such as formation stability theory, convergence, robot dynamics, environmental uncertainty models, and actuator saturation effects are not stressed. In work most closely related to this paper, Wang [8] developed dynamics models and control laws for robots in formation using full knowledge of the environment. He also presented proofs of formation stability in known conditions. He did not consider environmental uncertainty or adaptive behavior.

PROBLEM FORMULATION

Preliminaries

Consider N mobile autonomous robots living in a two-dimensional real Euclidean space denoted by \mathcal{R}^2 . The origin of \mathcal{R}^2 coincides with an inertial frame. This inertial frame is defined with a fixed orthonormal basis, $\mathcal{I} = (\mathbf{e}_x, \mathbf{e}_y)$. In our notation, a bold symbol

represents a vector quantity; otherwise the quantity is a scalar. Any point, \mathbf{r} , in the inertial frame can be represented as $\mathbf{r} = x\mathbf{e}_x + y\mathbf{e}_y$, or equivalently by the double $(x, y)_{\mathcal{I}}$. Each robot is represented by a point mass whose position at time t is given by $\mathbf{r}_n(t) = x_n(t)\mathbf{e}_x + y_n(t)\mathbf{e}_y$, $n = 1, 2, \dots, N$.

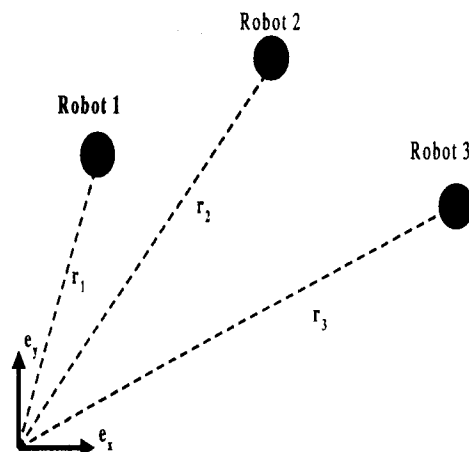


Figure 1: Three robot ($N=3$) formation.

Robot Equations of Motion

In free space, the equation of motion for each robot is given by

$$m_n \ddot{\mathbf{r}}_n(t) = \mathbf{F}^{\text{control}}_n(t) + \mathbf{F}^{\text{environ}}_n(t) \triangleq \mathbf{F}_n(t) \quad (1)$$

where m_n is the mass of the n th robot, $\mathbf{F}^{\text{control}}_n(t)$ is the force used to explicitly control the robot, $\mathbf{F}^{\text{environ}}_n(t)$ is force from the external environment, and $\ddot{\mathbf{r}}_n(t)$ denotes double differentiation with respect to time in inertial frame \mathcal{I} . $\dot{(\cdot)}$ denotes differentiation with respect to time. The robots may have a variety of sensors mounted on them. These provide sensory inputs or measurements. For example, a GPS receiver may measure position, a wheel encoder may measure speed, or an accelerometer may measure acceleration. Define the state vector of a robot as its position and velocity; then the state space equation for a single ro-

bot is

$$\begin{bmatrix} \ddot{\mathbf{r}}_n(t) \\ \dot{\mathbf{r}}_n(t) \\ \mathbf{r}_n(t) \end{bmatrix} = \begin{bmatrix} 0 & 1 \\ 0 & 0 \end{bmatrix} \begin{bmatrix} \mathbf{r}_n(t) \\ \dot{\mathbf{r}}_n(t) \end{bmatrix} + \begin{bmatrix} 0 \\ 1 \end{bmatrix} \mathbf{F}_n(t)/m_n \quad (2)$$

Note that equation (2) is simply equation (1) rewritten.

Environmental Friction Model

The simplest friction model available is that of a force in a direction opposite to the velocity of the robot,

$$\mathbf{F}^{\text{environ}} = -\rho_n \dot{\mathbf{r}}_n(t) \quad (3)$$

where ρ_n is a positive friction coefficient. The interaction of the friction model (environment) and the robot dynamics model takes the form of

$$m_n \ddot{\mathbf{r}}_n(t) + \rho_n \dot{\mathbf{r}}_n(t) = \mathbf{F}_n^{\text{control}}(t) \triangleq \mathbf{u}_n(t) \quad (4)$$

Formation Tracking Error

Let robot N be designated as the leader robot. The goal of any formation-keeping is to maintain a specific robot pattern with respect to this robot. Let robot N trace out a pre-determined differentiable path, $\mathbf{r}_N(t)$. Robot $(N-1)$'s desired path, $\mathbf{d}_{N-1}(t)$, is defined with respect to $\mathbf{r}_N(t)$,

$$\mathbf{d}_{N-1}(t) = \mathbf{r}_N(t) + \mathbf{q}_{N-1}(t) \quad (5)$$

where $\mathbf{q}_{N-1}(t)$ is called the deviation vector. The tracking error $\mathbf{e}_{N-1}(t)$ between the desired path and the actual path is given by

$$\mathbf{e}_{N-1}(t) = \mathbf{d}_{N-1}(t) - \mathbf{r}_{N-1}(t) \quad (6)$$

Without loss of generality, we will assume that the masses, $m_1 = \dots = m_{N-1} = m_N \triangleq 1$. Then, it can be shown that the error evolution is given by

$$\begin{aligned} \ddot{\mathbf{e}}_{N-1}(t) + \rho_{N-1} \dot{\mathbf{e}}_{N-1}(t) &= (\rho_{N-1} - \rho_N) \dot{\mathbf{r}}_N(t) + \ddot{\mathbf{q}}_{N-1}(t) + \\ &\quad \rho_{N-1} \dot{\mathbf{q}}_{N-1}(t) - \mathbf{u}_{N-1}(t) + \mathbf{u}_N(t) \end{aligned} \quad (7)$$

Equ. (7) may be used to motivate controllers that drive the error to zero.

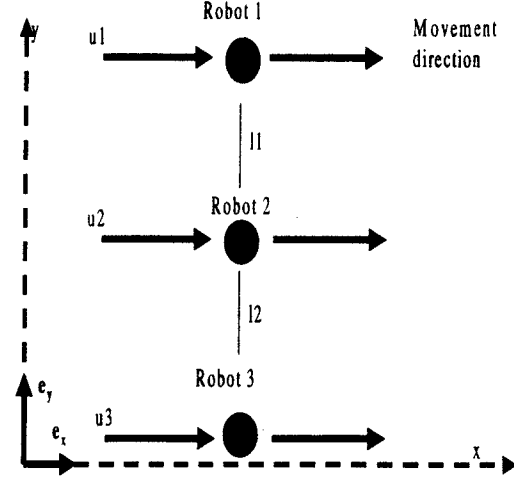


Figure 2: Three robots in Line Formation.

Three-Robot Line Formation Problem

Consider the formation-keeping task shown in figure 2. Each robot can move only in the $+x$ direction. Robot 3 is designated the *leader* robot. Robot 2 must maintain a y direction distance of l_2 from Robot 3, and Robot 1 must maintain a y direction distance of l_1 from Robot 2. The input forces are only applied in the $+x$ direction. In keeping with the notation of the previous subsections,

$$\mathbf{r}_3(t) \triangleq \begin{bmatrix} r_3(t) \\ 0 \end{bmatrix}; \mathbf{r}_2(t) \triangleq \begin{bmatrix} r_2(t) \\ 0 \end{bmatrix}; \mathbf{r}_1(t) \triangleq \begin{bmatrix} r_1(t) \\ 0 \end{bmatrix}; \quad (8)$$

$$\mathbf{q}_1(t) \triangleq \begin{bmatrix} 0 \\ l_1 \end{bmatrix}; \mathbf{q}_2(t) \triangleq \begin{bmatrix} 0 \\ l_2 \end{bmatrix} \quad (9)$$

$$\mathbf{u}_1(t) \triangleq \begin{bmatrix} u_1(t) \\ 0 \end{bmatrix}; \mathbf{u}_2(t) \triangleq \begin{bmatrix} u_2(t) \\ 0 \end{bmatrix}; \mathbf{u}_3(t) \triangleq \begin{bmatrix} u_3(t) \\ 0 \end{bmatrix} \quad (10)$$

$$\mathbf{e}_2(t) \triangleq r_3(t) - r_2(t); \mathbf{e}_1(t) \triangleq r_2(t) - r_1(t) \quad (11)$$

Note that for any static formation geometry, including a line formation, $\mathbf{q}_2(t)$ and $\mathbf{q}_1(t)$ are constant. Therefore, $\dot{\mathbf{q}}_{1,2}(t)$ and $\ddot{\mathbf{q}}_{1,2}(t)$ are also zero. These conditions turn the problem into a scalar problem of determining scalar control forces $u_3(t)$, $u_2(t)$ and $u_1(t)$ in the x direction. Errors in this case are the relative x -positions of the robots over time. Ideally, all robots should maintain the exact same x position over time.

FORMATION CONTROL

Control with Full Knowledge

The goal of the formation keeping task is to keep $\mathbf{e}_1(t)$ through $\mathbf{e}_{n-1}(t)$ as small as possible (ideally zero). By considering the form of (7), Wang [8] suggested that the control could be given by

$$\begin{aligned} \mathbf{u}_{n-1}(t) \triangleq & K_{n-1}\mathbf{e}_{n-1}(t) + \overline{K}_{n-1}\dot{\mathbf{e}}_{n-1}(t) + \\ & (\rho_{n-1} - \rho_n)\dot{\mathbf{r}}_n(t) + \ddot{\mathbf{q}}_{n-1}(t) + \rho_{n-1}\dot{\mathbf{q}}_{n-1}(t) + \mathbf{u}_n(t) \end{aligned} \quad (12)$$

where K_{n-1} is a positive constant used for proportional control and \overline{K}_{n-1} is a positive constant used for derivative control. In this case, (7) reduces to

$$\ddot{\mathbf{e}}_{n-1}(t) + (\rho_{n-1} + \overline{K}_{n-1})\dot{\mathbf{e}}_{n-1}(t) + K_{n-1}\mathbf{e}_{n-1}(t) = 0 \quad (13)$$

There exist infinitely many \overline{K}_{n-1} and K_{n-1} such that as $t \rightarrow \infty$, $\mathbf{e}_{n-1}(t) \rightarrow 0$, implying asymptotic stability. A formal proof of this fact is given by Wang [8].

Although elegant in mathematics, consider the knowledge required to implement (12). $\mathbf{e}_{n-1}(t)$ and $\dot{\mathbf{e}}_{n-1}(t)$ may be obtained by sensors mounted on the robots. $\dot{\mathbf{q}}_{n-1}(t)$ and $\ddot{\mathbf{q}}_{n-1}(t)$ may be computed a-priori. More difficult but possibly, $\dot{\mathbf{r}}_n(t)$ and $\mathbf{u}_n(t)$ in (12) may be transmitted from Robot n to Robot $(n-1)$. Most difficult, if not impossible, is the knowledge of ρ_{n-1} and ρ_n . This is because friction coefficients are not just a property of the robots themselves, but a property of the robot/terrain *interaction*. This terrain may change in the course of the robots or may be unknown as in the case of planetary rovers on other planets. Therefore, we must find some way to account for these changes in our controller.

Imperfect Knowledge

We now consider the formation error growth when friction and error control terms in (12) in the controller are incorrect. This could be the case when rovers are placed on planets whose surfaces are not well characterized. Consider the specific case where ρ_2 and ρ_3 are guessed to be 1.0 and 4.0 respectively. The true values of ρ_2 and ρ_3 are in reality 4.0 and 1.0 as in the previous subsections. The control (12) becomes

$$u_2(t) \triangleq e_2(t) + \dot{e}_2(t) + u_3(t) - 3.0\dot{r}_n(t) \quad (14)$$

The error equation (7) becomes

$$\ddot{e}_2(t) + 5.0\dot{e}_2(t) + e_2(t) = 6.0\dot{r}_3(t) \quad (15)$$

The explicit solution of this equation is

$$\begin{aligned} e_2(t) = & \frac{6}{5} + \left(-\frac{3}{5} - \frac{\sqrt{21}}{7}\right)e^{\frac{1}{2}(-5+\sqrt{21})t} - \\ & \frac{1}{35}(-5 + \sqrt{21})\sqrt{21}e^{-\frac{1}{2}(5+\sqrt{21})t} \end{aligned} \quad (16)$$

Figure 3 shows the growth of position error.

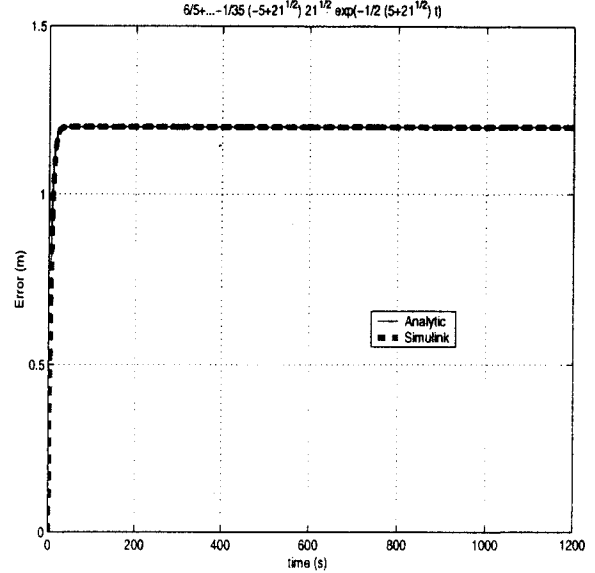


Figure 3: Position error (e_2) in x direction between Robot 3 and Robot 2. Imperfect Knowledge of Friction-Dependent Control Terms. System is still not asymptotically stable and error has increased.

Adaptive Robot Controller

Direct Adaptive Controller

Define a new variable,

$$\gamma_{n-1} \triangleq \rho_{n-1} - \rho_n \quad (17)$$

Assume that γ_{n-1} may be estimated through the use of a parameter estimator. Then, by using this estimate, we implement a new adaptive controller of the form

$$\begin{aligned} u_{n-1}(t) \triangleq & K_{n-1}e_{n-1}(t) + \overline{K}_{n-1}\dot{e}_{n-1}(t) + \\ & \widehat{\gamma}_{n-1}(t)\dot{r}_n(t) + u_n(t) \end{aligned} \quad (18)$$

where \overline{K}_n is a positive constant used for derivative control and K_{n-1} is a positive constant used for proportional control.

Direct Adaptive Estimator

Let the estimate of γ_{n-1} be governed by the following update equation,

$$\dot{\hat{\gamma}}_{n-1}(t) = -P_{12}e_{n-1}(t)\dot{r}_n(t) - \dot{e}_{n-1}(t)\dot{r}_n(t) \quad (19)$$

where the scalar parameter P_{12} is such that

$$\overline{K_{n-1}} \geq \sqrt{K_{n-1}} > P_{12} > 0 \quad (20)$$

Direct Adaptive Lyapunov Stability

Theorem

Let robot N (leader) employ a stable controller. Let robots $1 \dots (N-1)$ use the controller given in (18) and the estimator given in (19); then the overall formation is asymptotically stable such that, for $n = 1 \dots N-1$, $e_{n-1} \rightarrow 0$, $t \rightarrow \infty$.

Proof

The strategy of the proof is to use Barbalat's Lemma to show $\dot{V}_{n-1}(e_{n-1}^2, \dot{e}_{n-1}^2, t) \rightarrow 0$ as $t \rightarrow \infty$. This will imply $e_{n-1}, \dot{e}_{n-1} \rightarrow 0$ as $t \rightarrow \infty$, showing $e_{n-1} = 0$ is asymptotically stable.

Recall Barbalat's Lemma [10]: If a scalar function $V(\mathbf{x}, t)$ is such that

- (BL1) $V(\mathbf{x}, t) \geq 0$
- (BL2) $\dot{V}(\mathbf{x}, t) \leq 0$
- (BL3) $\dot{V}(\mathbf{x}, t)$ is uniformly continuous

Then $\dot{V}(\mathbf{x}, t) \rightarrow 0$ as $t \rightarrow \infty$.

Choose

$$V_{n-1}(e, \dot{e}, \gamma, t) \triangleq \frac{1}{2}\mathcal{E}^T \mathcal{P} \mathcal{E} + \frac{1}{2}(\gamma_{n-1} - \widehat{\gamma}_{n-1})^2 \quad (21)$$

where

$$\mathcal{E} \triangleq \begin{bmatrix} e_{n-1} \\ \dot{e}_{n-1} \end{bmatrix} \quad (22)$$

and

$$\mathcal{P} \triangleq \begin{bmatrix} K_{n-1} + P_{12}\rho_{n-1} + P_{12}\overline{K_{n-1}} & P_{12} \\ P_{12} & 1 \end{bmatrix} \quad (23)$$

Imposing the conditions in \mathcal{P} that

- (Pf1) $P_{12} > 0$

- (Pf2) $K_{n-1} > P_{12}^2$

implies $V_{n-1} \geq 0$ to satisfy (BL1). Now using (7) and (18)

$$\begin{aligned} \dot{V}_{n-1} = & (-\rho_{n-1} - \overline{K_{n-1}} + P_{12})\dot{e}_{n-1}^2 - K_{n-1}P_{12}e_{n-1}^2 + \\ & (\gamma_{n-1} - \widehat{\gamma}_{n-1})(\dot{r}_n\dot{e}_{n-1} + P_{12}\dot{r}_ne_{n-1} + \dot{\gamma}_{n-1} - \dot{\widehat{\gamma}}_{n-1}) \end{aligned} \quad (24)$$

Substituting for $\dot{\widehat{\gamma}}_{n-1}$ from (19) and imposing the condition

- (Pf3) $\overline{K_{n-1}} > P_{12}$

implies

$$\dot{V}_{n-1} = (-\rho_{n-1} - \overline{K_{n-1}} + P_{12})\dot{e}_{n-1}^2 - K_{n-1}P_{12}e_{n-1}^2 \leq 0 \quad (25)$$

satisfying (BL2). Note that (Pf1)-(Pf3) are equivalent to (20). In order to show $\dot{V}_{n-1}(e_{n-1}, \dot{e}_{n-1}, t)$ is uniformly continuous, we note that $|\ddot{V}_{n-1}| < \infty$ is a sufficient condition for uniform continuity.

$$\begin{aligned} |\ddot{V}_{n-1}| = & |2(-\rho_{n-1} - \overline{K_{n-1}} + P_{12})\dot{e}_{n-1}\ddot{e}_{n-1}| - \\ & |2K_{n-1}P_{12}e_{n-1}\dot{e}_{n-1}| \\ \leq & |2(-\rho_{n-1} - \overline{K_{n-1}} + P_{12})||\dot{e}_{n-1}||\ddot{e}_{n-1}| \\ & - |2K_{n-1}P_{12}||e_{n-1}||\dot{e}_{n-1}| \end{aligned} \quad (26)$$

The fact that $(V_{n-1} \geq 0)$ and $(\dot{V}_{n-1} \leq 0)$ implies

- $|e_{n-1}| < \infty$
- $|\dot{e}_{n-1}| < \infty$
- $|\gamma_{n-1} - \widehat{\gamma}_{n-1}| < \infty$

Recall

$$\ddot{e}_{n-1} = (-\rho_{n-1} - \overline{K_{n-1}})\dot{e}_{n-1} + (\gamma_{n-1} - \widehat{\gamma}_{n-1})\dot{r}_n - K_{n-1}e_{n-1} \quad (27)$$

Then

$$\begin{aligned} |\ddot{e}_{n-1}| \leq & |(-\rho_{n-1} - \overline{K_{n-1}})||\dot{e}_{n-1}| + \\ & |(\gamma_{n-1} - \widehat{\gamma}_{n-1})||\dot{r}_n| - \\ & |K_{n-1}||e_{n-1}| < \infty \end{aligned} \quad (28)$$

Therefore

$$|\ddot{V}_{n-1}| < \infty \quad (29)$$

satisfying (BL3). Therefore

$$\dot{V}_{n-1} = (-\rho_{n-1} - \overline{K_{n-1}} + P_{12})\dot{e}_{n-1}^2 - K_{n-1}P_{12}e_{n-1}^2 \rightarrow 0 \quad (30)$$

as $t \rightarrow \infty$. Therefore, $e_{n-1} = 0$ is asymptotically stable. QED.

Note that (Pf1)-(Pf3) determine the selection of P_{12} . However, for any K_{n-1} , $\overline{K_{n-1}} > 0$, $\exists P_{12}$ that satisfies (Pf1)-(Pf3).

Direct Adaptive Example

Returning to the three robot example of the last section, consider the error given an input of

$$u_2(t) \triangleq e_2(t) + \dot{e}_2(t) + \widehat{\gamma_2(t)}\dot{r}_3(t) + u_3(t) \quad (31)$$

and estimator of the form

$$\dot{\gamma}_2(t) = -0.9e_2(t)\dot{r}_3(t) - \dot{e}_2(t)\dot{r}_3(t) \quad (32)$$

Figure 4 shows the growth of position error. Clearly, this controller has stabilized the system.

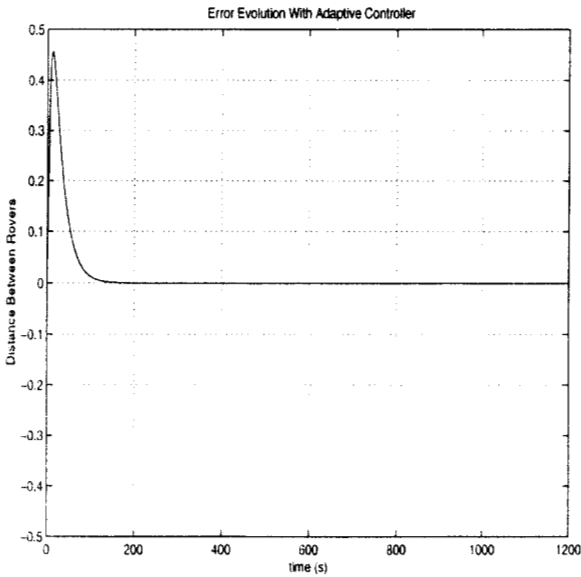


Figure 4: Position error (e_2) in x direction between Robot 3 and Robot 2. Adaptive controller has stabilized the system.

EFFECT OF ACTUATOR SATURATION

Effect of Actuator Saturation

Consider two identical robots oriented side to side and moving forward. Suddenly, the nature of the terrain under one robot changes to a much more difficult condition, but the terrain under the other robot remains the same. In order to maintain a rigid formation, the robot in the more difficult terrain must increase its control energy in order to compensate for the more difficult terrain. A situation may arise, however, that the terrain is so difficult that the follower robot's controller is saturated. In this case, the follower robot will fall further and further behind the leader as time goes on.

For the two robot line formation case, this situation is illustrated in figure 5. Robot 2 (follower) and robot 3

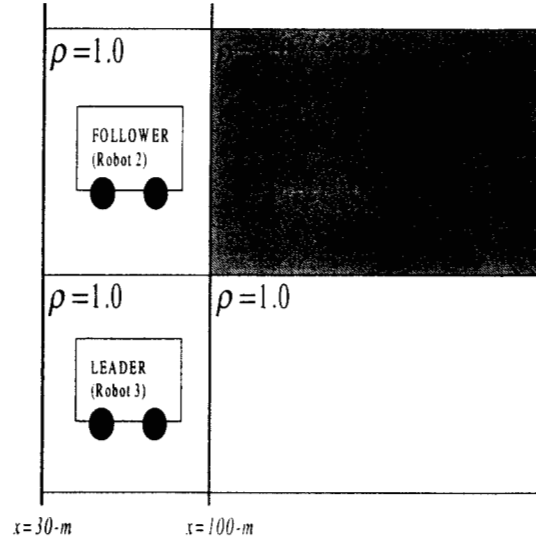


Figure 5: Change in terrain under one robot of a 2-robot line formation.

(leader) start at $x = 30$ and encounter the same friction coefficient ($\rho_{2,3} = 1.0$) until $x = 100$ -m. At that position, robot 2's terrain changes to a friction coefficient ($\rho_2 = 4.0$) four times robot 3's friction coefficient ($\rho_3 = 1.0$). Figure 6 shows robot 2's desired control force in order to keep the line formation and compensate for the increased friction. From the last section, robot 2's adaptive controller identifies the new terrain and the positional error goes to zero.

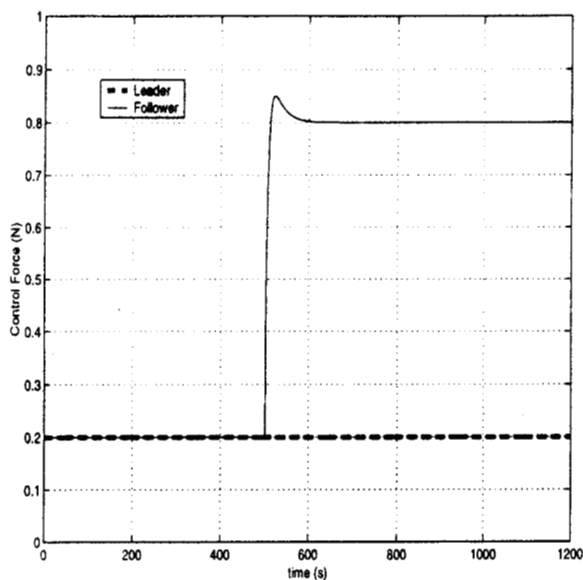


Figure 6: Change in control force with increased friction and infinite available control force.

Now consider the case in which each robot's locomotion motor saturates at $u = .5$ -Newtons. In this case, robot 2's controller tries to compensate, but ends up pinned at the upper saturation limit (figure 7). Since

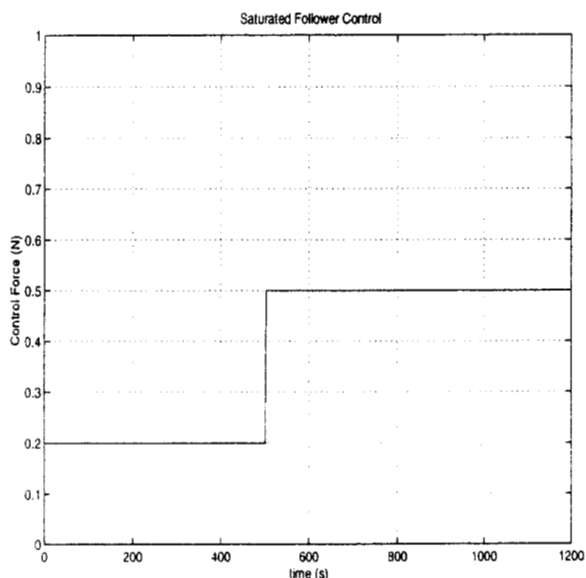


Figure 7: Control force of robot 2 with actuator saturation. Controller would like to mimic control force of fig. 6, but instead gets pinned at upper limit.

the controller is unable to produce the force needed, robot 3 soon pulls away from robot 2 and the line

formation error (fig. 8) increases without bound.

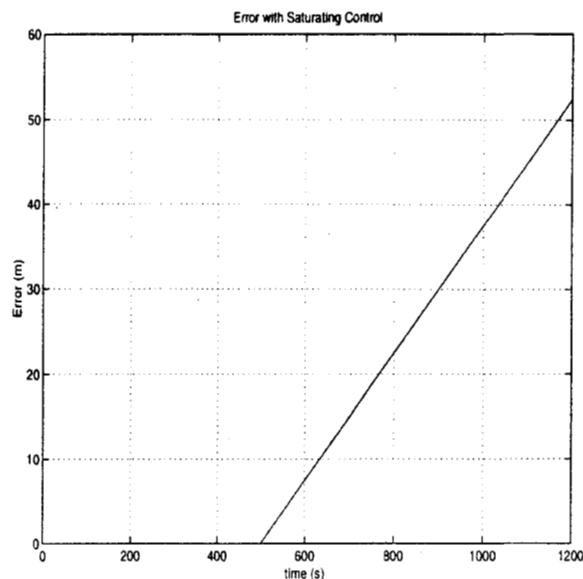


Figure 8: Error between robot 2 and robot 3 with finite available control force. Robot 3 pulls away from robot 2.

Ethological Control Solution

In order to understand a possible solution to this problem, consider what people may do under the same conditions. In fact, this situation occurs often in a slightly different circumstance. Frequently, two people are walking side by side and one person naturally tends to walk faster. The other member of the couple tries to keep up until the point where their energy is spent. At this point, the faster person pulls ahead. At some time, the faster person is so far ahead that the slower person must yell, "STOP!". The faster person then stops and waits for the slower person to "catch up." Then, the couple resumes their walking, but now the faster person slows their speed as compared to their previous speed. We may mimic this same control strategy for robots, as well as extend it for N robots in a line formation.

Group Adaptation

Control Algorithm

Consider N robots in a line formation. Nominally, the adaptive control mechanisms from section are implemented. Robot N is the leader and sets a target speed

for the entire formation. However, if robot $n - 1$ falls behind robot n by a preset tolerance (due to e.g. actuator saturation), robot $n - 1$ transmits a signal to robot n to stop. In this case, robot n also transmits a signal to robot $n + 1$ to stop. Similarly, all robots from n to N stop. These robots continue to stop until robot $n - 1$ regains alignment with robot n . Note that since robot $n - 2$'s control is dependent on robot $n - 1$'s actions, all robots from 1 to $n - 1$ will stay in line. Once robot $n - 1$ regains alignment, robot $n - 1$ stops (as then do all robots from 1 to $n - 1$). At this stage, all robots are stopped and the formation is re-initialized. Robot n transmits a signal to robot $n + 1$ that all robots less than n are now ready and aligned. Similar transmissions occur until robot N is informed all robots are ready. At this stage, robot N lowers its speed and the entire formation starts moving again. Note that all communication occurs only with the robot to the right. Also note that only robot N (leader) explicitly lowers its target speed. This control strategy has been constructed in simulation via finite state machines.

Weakest Link Behavior

If, even after robot N 's speed is reduced, one robot falls behind again, the whole procedure starts again until robot N 's speed is reduced yet again. The overall effect of this procedure is that the entire robot formation eventually *adapts* to the slowest robot. In this way, the entire formation is now adaptive just as the individual robots are adaptive. Let us return to the example of last section. Figure 9 shows the new error profile of using the ethological control scheme. The robots start out in formation and remain in formation until the terrain under the follower changes. At this time, because of actuator saturation in robot 2, robot 3 pulls away and the error between the two robots gets larger with time. Eventually, the error gets so large that robot 3 is instructed to stop. At this point, robot 2 starts catching up and the error between the two robots decreases. Finally, the robots are in line. Robot 3 lowers its target speed and the two robots start up again. Robot 3's speed is still too fast for robot 2 to keep up. As a result, robot 2's input is again saturated and the error again starts to increase. Note however, that the *rate* of error increase has decreased. This is due to robot 3's lower speed. Again, the error increases until robot 3 is again instructed to stop. When robot 2 again catches up, robot 3's speed is reduced again. At this speed, robot 2's control is no longer saturated and the error between the two falls to

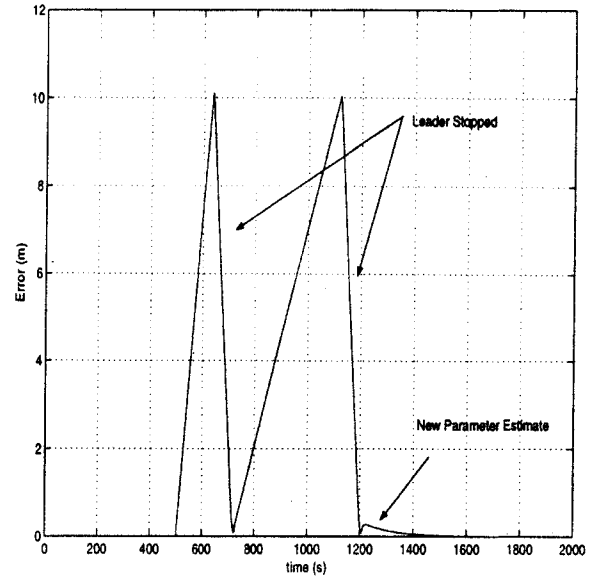


Figure 9: Error between robot 2 and robot 3 within ethological control strategy. $K_1 = K_2 \triangleq 1$, $\overline{K}_1 = \overline{K}_2 \triangleq 1$, $P_{12} \triangleq 0.9$.

zero. The hump in the error profile is caused by convergence to a new gamma estimate. Figure 10 shows the velocity of robot 3 during this process. Note that the velocity falls to lower and lower levels until the entire formation has adapted to its highest sustainable speed.

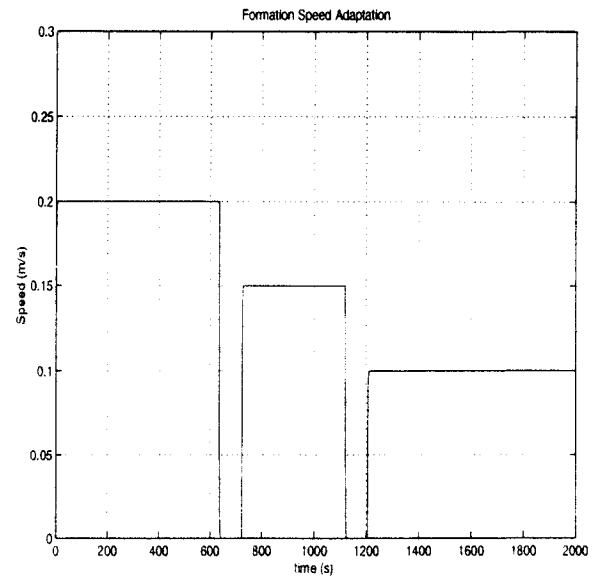


Figure 10: Adaptation of leader robot speed to highest sustainable speed.

CONCLUSIONS

This paper studied adaptive behavior within multi-agent autonomous robot formation-keeping. It was shown that adaptation can occur at several different levels in a formation control architecture; just as a single robot may adapt to a new environment, a robot-formation as a whole may also adapt to a new environment. Terrain uncertainty and related actuator saturation were identified as important limitations to formation-keeping in uncertain environments. In order to account for terrain uncertainty, individual robots were equipped with parameter estimators to allow implementation of direct adaptive control. Using these adaptive controllers, it was shown that formation error reduces to zero under non-saturated conditions. Actuator saturation brings new challenges to formation-keeping. It was shown that a difficult terrain can easily lead to actuator saturation. For this case, a new ethological control scheme was introduced. It was shown that in this case the entire formation adapted to the weakest robot.

References

- [1] T. Huntsberger, G. Rodriguez, and P.S. Schenker "Robotics Challenges for Human and Robotic Mars Exploration," *Proceedings of the Space 2000 Conference*, Albuquerque, New Mexico, 2000.
- [2] R.D. Beer, "The Dynamics of Adaptive Behavior: A Research Program," *Robotics and Autonomous Systems*, Vol. 20, 1997, pp. 257-289.
- [3] T.L. Dean and M.P. Wellman, *Planning and Control*, Morgan-Kaufmann, New York, 1991.
- [4] L.E. Parker, "Designing Control Laws for Cooperative Agent Teams," *Proceedings of the 1993 IEEE International Conference on Robotics and Automation*, 1993, pp. 582-587.
- [5] L.E. Parker, "Heterogeneous MultiRobot Cooperation," *PhD Dissertation*, Department of Electrical Engineering and Computer Science, MIT, 1994.
- [6] T. Balch and R.C. Arkin "Behavior-Based Formation Control for Multirobot Teams," *IEEE Transactions on Robotics and Automation*, Vol. 14, No. 6, 1998, pp. 926-939.
- [7] M. Mataric "Reinforcement Learning in the Multi-Robot Domain," *Autonomous Robots*, Vol. 4, 1997, pp. 73-83.
- [8] P.K.C. Wang, "Navigation Strategies for Multiple Autonomous Mobile Robots Moving in Formation," *Journal of Robotic Systems*, Vol. 20, No. 2, 1991, pp. 177-195.
- [9] K.J. Astrom and B. Wittenmark, *Adaptive Control (2nd Edition)*, Addison-Wesley: Reading, MA, 1995.
- [10] J.J. Slotine and W. Lee, *Applied Nonlinear Control*, Prentice Hall: Englewood Cliffs, NJ, 1991.

Acknowledgments

I would like to acknowledge Dr. David S. Bayard of the Jet Propulsion Laboratory for assistance in the analysis of the direct adaptive controller.

This work was performed at the Jet Propulsion Laboratory, under a contract from the National Aeronautics and Space Administration. This work has been funded under the CETDP/Surface Systems Thrust and was performed within the Robot Work Crews (RWC) Task led by Dr. Paul S. Schenker at the Jet Propulsion Laboratory.